

## Raman spectroscopic studies of oxygen defects in Co-doped ZnO films exhibiting room-temperature ferromagnetism

This article has been downloaded from IOPscience. Please scroll down to see the full text article.

2007 J. Phys.: Condens. Matter 19 026212

(<http://iopscience.iop.org/0953-8984/19/2/026212>)

View [the table of contents for this issue](#), or go to the [journal homepage](#) for more

Download details:

IP Address: 129.252.86.83

The article was downloaded on 28/05/2010 at 15:20

Please note that [terms and conditions apply](#).

# Raman spectroscopic studies of oxygen defects in Co-doped ZnO films exhibiting room-temperature ferromagnetism

C Sudakar<sup>1</sup>, P Kharel<sup>1</sup>, G Lawes<sup>1</sup>, R Suryanarayanan<sup>1,3</sup>, R Naik<sup>1</sup> and V M Naik<sup>2</sup>

<sup>1</sup> Department of Physics and Astronomy, Wayne State University, Detroit, MI 48201, USA

<sup>2</sup> Department of Natural Sciences, University of Michigan-Dearborn, Dearborn, MI 48128, USA

E-mail: [sury39@yahoo.com](mailto:sury39@yahoo.com)

Received 19 August 2006, in final form 23 November 2006

Published 15 December 2006

Online at [stacks.iop.org/JPhysCM/19/026212](http://stacks.iop.org/JPhysCM/19/026212)

## Abstract

The optical properties, Raman spectra, and magnetization of  $\text{Zn}_{1-x}\text{Co}_x\text{O}$  ( $0 \leq x < 0.1$ ) thin films are reported. Optical transmission spectra confirm the substitution of  $\text{Co}^{2+}$  cations for  $\text{Zn}^{2+}$  ions at the tetrahedral sites of ZnO. Raman spectra of films annealed in air show an additional broad vibrational mode, attributed to disordered  $-\text{Zn}-\text{O}-\text{Co}-$  local vibrations. These modes disappear on vacuum annealing, suggesting the formation of oxygen vacancies close to the dopant sites ( $-\text{Zn}-\square-\text{Co}-$ ). Magnetization measurements show that air-annealed films lack significant moment, whereas vacuum-annealed samples with intermediate Co concentrations ( $0.012 < x < 0.05$ ) exhibit room-temperature ferromagnetism. Using the framework of the bound magnetic polaron model, the polaron size is estimated to be roughly  $7.8 \text{ \AA}$  for this system.

ZnO has attracted renewed interest because of its relevance to a wide range of applications in optical, piezoelectric devices and chemical sensors [1]. One technology where ZnO could have a major impact is the emerging field of spintronics based on diluted magnetic semiconductors (DMS) [2]. Dietl *et al* [3] predicted theoretically that ZnO-based DMS should exhibit room-temperature ferromagnetism (FM), initiating intensive research on ZnO doped with different 3d transition metals (TM = Co, Mn, Fe, Ni, Cr, etc). Following the original report by Ueda *et al* [4], many reports have appeared on Co-doped ZnO thin films exhibiting ferromagnetism with  $T_C$  above room temperature [5–9]. It remains an open question whether this ferromagnetic order is intrinsic to the Co-substituted ZnO system or arises from magnetic impurity clusters. The distribution of oxygen vacancies is believed to be a crucial component in the development of ferromagnetism in these systems [10]. To address properly the question

<sup>3</sup> Permanent address: LPCES, CNRS, ICMO, Université Paris-Sud, 91405 Orsay, France.

of whether oxygen vacancies could be responsible for room-temperature ferromagnetism in TM:ZnO films, it is necessary to correlate the magnetic properties of these films with other features that are characteristic of oxygen vacancies. Building on several studies on the role of lattice defects on the Raman spectra of undoped and doped (Li, N, Fe, Sb, Ga, and Al) ZnO films [11–13], we have used Raman spectroscopy to determine whether there are Raman modes that could be associated with TM–O vibrations which change as oxygen vacancies are created or destroyed.

In this paper we report the changes in the Raman spectra of Co:ZnO thin films that occur upon annealing the films alternately in air/high vacuum (HV), and discuss the results in relation to the magnetic properties of the samples. It has been suggested that oxygen vacancies play an important role in the development of ferromagnetism in doped semiconducting oxides, most notably in the bound magnetic polaron model [9]. HV annealing is expected to introduce oxygen vacancies ( $\square$  or  $V_O$ ), which are removed when the film is annealed in air. We confirm this prediction by using micro-Raman spectroscopy to monitor a –Zn–O–Co– related local vibrational mode, which switches on and off under air and HV annealing, respectively. The net magnetization of the films is also found to switch between the FM and non-magnetic values under these different annealing conditions. The highly reproducible changes in Raman spectra accompanying the magnetic switching suggest a connection between the presence of intrinsic  $V_O$  in the films and the occurrence of ferromagnetism.

$Zn_{1-x}Co_xO$  ( $0 \leq x < 0.1$ ) films of thickness  $\sim 0.5$ – $1 \mu\text{m}$  were prepared by the metalorganic decomposition (MOD) method on sapphire substrates. The method involves the preparation of precursor solutions using Zn 2-ethylhexanoate (liquid) and Co 2-ethylhexanoate (liquid) in appropriate proportions, and ultrasonically mixing the solution with the addition of a small amount of xylene to obtain the optimal viscosity needed for spin-coating. The  $Zn_{1-x}Co_xO$  films were prepared by dispensing the metalorganic precursor solution onto *c*-plane sapphire substrates ( $1$ – $2 \text{ cm}^2$ ), which were then spun at 5000 rpm for 15 s followed by baking the sample at  $550^\circ\text{C}$  for 1 min. The process was repeated between five and ten times to build up the desired layer thickness. The final annealing of the sample was done at  $700^\circ\text{C}$  in air for 60 min. These samples are referred to as ‘air annealed’ in the following text. In order to introduce oxygen vacancies into the films, the samples were annealed in high vacuum ( $10^{-5}$ – $10^{-6}$  Torr) at a temperature of  $550^\circ\text{C}$  for 1 h and are referred to as ‘HV annealed’. By comparing the magnetic behaviour of the same samples before and after vacuum annealing, the effect of oxygen vacancies on magnetization has been studied without changing the distribution of Co ions in the films.

The crystal structure and the phase formation of ZnO and  $Zn_{1-x}Co_xO$  thin films characterized by x-ray diffraction (XRD) reveals a single polycrystalline ZnO phase with wurtzite structure. No additional peaks were observed, indicating that there are no structural changes and/or formation of additional phases due to the incorporation of Co in ZnO within the limits of XRD detection.

The optical transmission spectra of  $Zn_{1-x}Co_xO$  thin films annealed in air (figure 1(a)) and in HV (figure 1(b)) were recorded using a Perkin–Elmer ultraviolet/visible (UV–vis) spectrometer (Lambda 900) in the 200–900 nm wavelength range. Besides the band-edge absorption, additional absorption peaks around 652, 611 and 566 nm are observed in all compositions of  $Zn_{1-x}Co_xO$  thin films. These localized absorption bands are attributed to a  $\text{Co}^{2+}$  interatomic d–d transition associated with the crystal-field splitting in the ZnO host due to transitions from  $^4A_2(\text{F})$  to  $^2E(\text{G})$ ,  $^4T_1(\text{P})$ , and  $^2A_1(\text{G})$  [14]. The observation of these transitions in the transmission spectra confirms the substitution of  $\text{Co}^{2+}$  cations for the  $\text{Zn}^{2+}$  ions at the tetrahedral sites of ZnO. The intensity of these bands increases with Co concentration in  $Zn_{1-x}Co_xO$  thin films, pointing to an increase in  $\text{Co}^{2+}$  ion concentration in the ZnO lattice

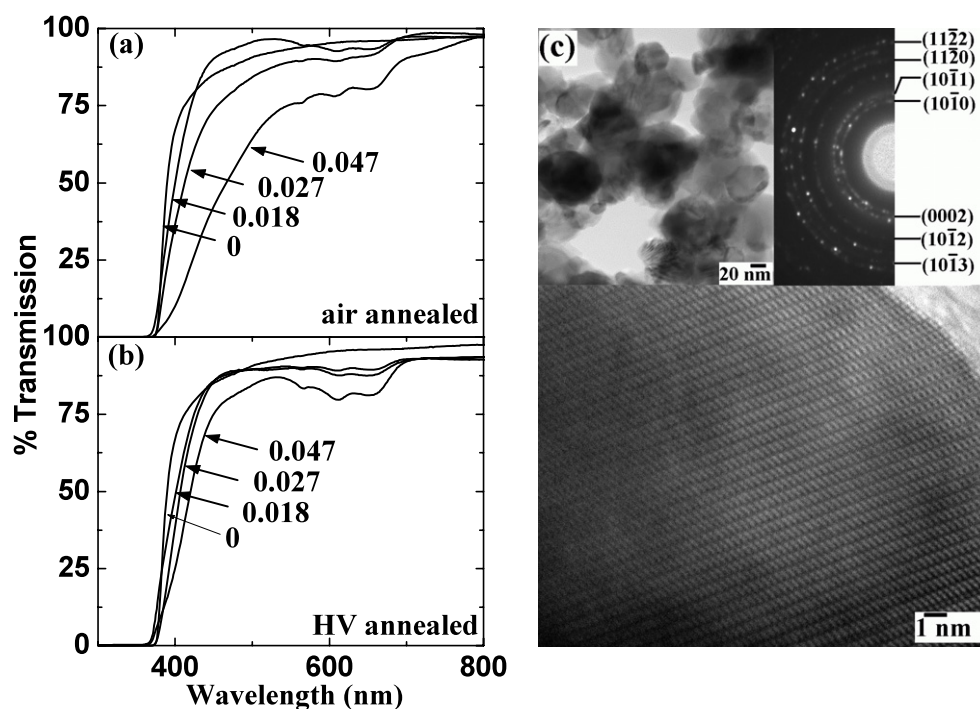


**Figure 1.** Optical transmission spectra of  $\text{Zn}_{1-x}\text{Co}_x\text{O}$  thin films annealed in (a) air and (b) high vacuum. (c) Bright-field image (top left), SAED (top right) and HRTEM image (bottom panel) of 4.7 at.% Co doped ZnO.

with increasing  $x$ . A significant difference in the band-edge slopes between the spectra of air- and HV-annealed samples is observed. The band edge shows a more diffuse transition for air-annealed samples, whereas the absorption edge becomes sharper on HV annealing the films. The band tailing is generally attributed to point defects such as  $\text{Co}_{\text{Zn}}$ , interstitial  $\text{Co}^{3+}$ , and zinc vacancies [15]. It is difficult to analyse the optical intensity quantitatively to ascertain the absence of Co clusters, as the absorption can also be due to other sources, including defects. In order to investigate the presence or absence of Co clusters in these samples, a thorough analysis using high-resolution transmission electron microscopy (HRTEM) imaging and selected area electron diffraction (SAED) was carried out. Figure 1(c) shows these details for a representative sample with higher Co concentration (4.7 at.%). Further, energy dispersive x-ray spectroscopy (EDXS) data using a focused electron probe for detailed compositional analyses on nanometre-scale particles indicated a solid solution of Co in the ZnO lattice. There was no evidence for the presence of Co metal or Co-rich regions within the films in any of these detailed TEM measurements. Further, concurrent studies on  $\text{Co}_{3-y}\text{Zn}_y\text{O}_4$  films show only  $\text{Co}_{1-x}\text{Zn}_x\text{O}$  phase formation on HV annealing with no detectable Co metal clusters using any of the above techniques.

The Raman spectra were recorded at room temperature with a Renishaw 1000 micro-Raman system using a 514.5 nm (2.41 eV) excitation line from an  $\text{Ar}^+$ -ion laser. The Raman scattering geometry used  $[z(x+y, x+y)\bar{z}]$  in the experiments allows the observation of  $E_2$  (low),  $E_2$  (high) and  $A_1$  (LO) phonon modes of the hexagonal wurtzite ZnO. The Raman spectra of  $\text{Zn}_{1-x}\text{Co}_x\text{O}$  films show all the expected ZnO phonon modes for  $x = 0$  [16]. As shown in figure 2, in addition to the phonon modes from the sapphire substrate (marked by \*),

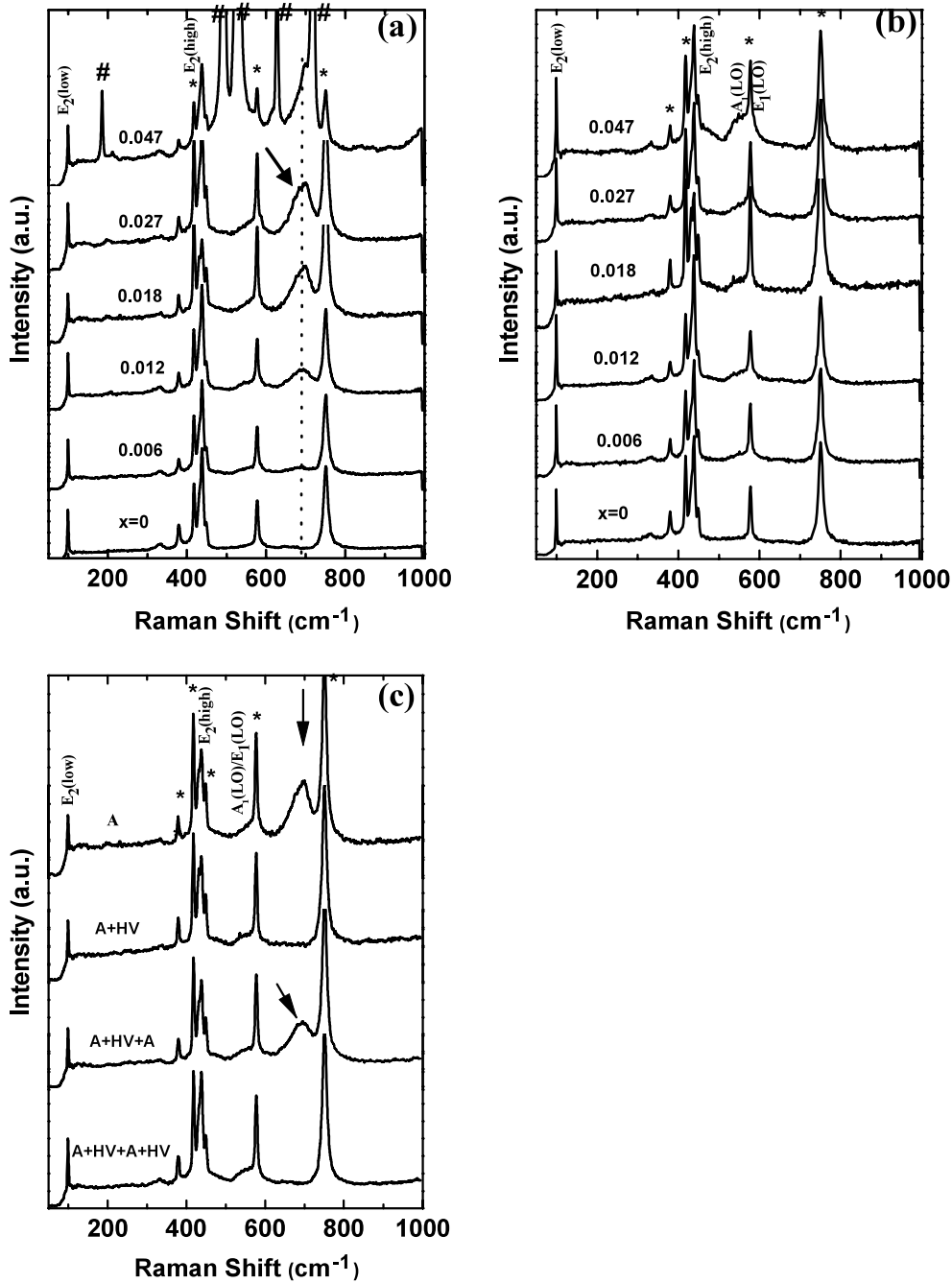


**Figure 2.** Raman spectra of  $Zn_{1-x}Co_xO$  thin films annealed in (a) air and (b) high vacuum. The peaks labelled with \* and # originate from the sapphire substrate and the  $Zn_yCo_{3-y}O_4$  clusters. The arrow points to the disorder activated mode. (c) Raman spectra of  $Zn_{0.982}Co_{0.018}O$  thin film subjected to repeated annealing in air (A) and high vacuum (HV).

two additional modes were observed at 99.7 and 438  $cm^{-1}$ . These modes are assigned to  $E_2$  (low) at 100  $cm^{-1}$  and  $E_2$  (high) at 438  $cm^{-1}$  for standard ZnO in [16]. The other expected

modes for ZnO are  $E_1$  (LO) = 583  $\text{cm}^{-1}$ ,  $E_1$  (TO) = 407  $\text{cm}^{-1}$ ,  $A_1$  (LO) = 574  $\text{cm}^{-1}$ , and  $A_1$  (TO) = 380  $\text{cm}^{-1}$ . However, sapphire substrate also has overlapping Raman modes at 576, 417 and 380  $\text{cm}^{-1}$ . As the Co concentration in ZnO increases, a broad impurity mode at  $\sim 690 \text{ cm}^{-1}$  develops in the air-annealed samples (figure 2(a)). As  $x$  increases, the intensity of this band increases and, for films with  $x \geq 0.047$ , very strong additional bands are observed at 186, 491, 526, 628 and 718  $\text{cm}^{-1}$  (marked by # in figure 2(a)). These additional bands may be assigned to complexes such as  $\text{Zn}_y\text{Co}_{3-y}\text{O}_4$ , as these bands are similar to  $\text{Co}_3\text{O}_4$  or  $\text{ZnCo}_2\text{O}_4$  spinel structure [17, 18].  $\text{Zn}_y\text{Co}_{3-y}\text{O}_4$  clusters are too small to be detected by XRD, but show up clearly in Raman scattering. In the low-Co-concentration ( $x < 0.047$ ) samples, the broad impurity band around 690  $\text{cm}^{-1}$  can be associated with disordered local vibrational modes (LVM) of  $-\text{Co}-\text{O}-\text{Zn}-$  in ZnO, based on the observation that this mode is absent in pure ZnO and that also the intensity ratio of LVM (690  $\text{cm}^{-1}$ )/ $E_2$  (high) increases with increasing  $x$ . This assignment is consistent with our expectation that the LVM of  $-\text{Co}-\text{O}-\text{Zn}-$  in ZnO should be detected at higher wavenumber than the highest phonon frequency of ZnO because of the smaller mass of Co compared to Zn [19]. Further investigations and modeling will be required for a definitive assignment of this mode.

On annealing the samples in high vacuum, the impurity band at 690  $\text{cm}^{-1}$  in all samples and also the strong peaks associated with  $\text{Zn}_y\text{Co}_{3-y}\text{O}_4$  vanish, leaving only the phonon modes characteristic of ZnO (figure 2(b)). These bands reappear on annealing in air at 700 °C for 1 h (albeit with a smaller intensity) and again disappear on second high-vacuum annealing, demonstrating a switching behaviour between the two states, as illustrated in figure 2(c) for  $\text{Zn}_{0.982}\text{Co}_{0.018}\text{O}$  sample. The switching in  $\text{Zn}_{1-x}\text{Co}_x\text{O}$  ( $0 \leq x < 0.1$ ) thin films is highly reproducible. These observations suggest that the 690  $\text{cm}^{-1}$  mode is related not only to the presence of the dopant ions, but also to the intrinsic lattice defects surrounding these ions.

We interpret these results as follows: oxygen vacancies are created when the films are annealed under high vacuum. A local lattice rearrangement takes place in the sample, leaving a larger concentration of  $V_{\text{O}}$  defects close to the Co ions in the lattice. The activation energy required to develop and diffuse oxygen vacancies through ZnO is  $\sim 0.07 \text{ eV}$  [20], so we expect a significant  $V_{\text{O}}$  diffusion at 550 °C. Postulating that the 690  $\text{cm}^{-1}$  Raman active mode is related to disordered  $-\text{Zn}-\text{O}-\text{Co}-$  vibrations, this excitation would be strongly suppressed when  $V_{\text{O}}$  defects cluster about Co ions, i.e.  $-\text{Zn}-\square-\text{Co}-$ . In the case of the Co-doped  $\text{TiO}_2$  system, calculations predict that the oxygen vacancies are more likely to occur near the Co sites than the Ti sites [21]. A similar mechanism could increase the concentration of  $V_{\text{O}}$  close to Co sites compared to the Zn sites. When the sample is annealed in air, the  $V_{\text{O}}$  defects are annealed out as additional oxygen enters the system. These annealing conditions are not sufficiently extreme to promote Co clustering inside the ZnO matrix, as evidenced by the optical absorption spectrum showing that Co remains incorporated in ZnO lattice in the 2+ state.

We now discuss the magnetic properties of these  $\text{Co}_x\text{Zn}_{1-x}\text{O}$  films under both air annealing and HV annealing. A superconducting quantum interference device (SQUID) magnetometer was used to measure magnetization ( $M$ ) versus applied magnetic field ( $H$ ) at 300 K.  $M$  as a function of  $H$  ( $-5$  to  $+5$  kOe) of the blank substrate was also measured in order to eliminate this diamagnetic contribution. We note that non-zero values of  $M$  upon HV annealing the sapphire substrates on the order of  $\sim 10^{-5}$  emu (absolute) were observed. The origin of this moment is unclear, however this value is much smaller (by more than an order of magnitude) than the Co-doped ZnO films and does not significantly affect the results presented here. The upper panel of figure 3 shows the substrate-corrected value of  $M$  versus  $H$  at  $T = 300 \text{ K}$  for a  $\text{Co}_{0.012}\text{Zn}_{0.988}\text{O}$  film, under both air-annealed and vacuum-annealed conditions. The lower panel of figure 3 shows the room-temperature  $M$  of  $\text{Zn}_{1-x}\text{Co}_x\text{O}$  ( $0 < x < 0.1$ ) films annealed in air and in HV. The dashed lines are a guide to the eye, illustrating the change

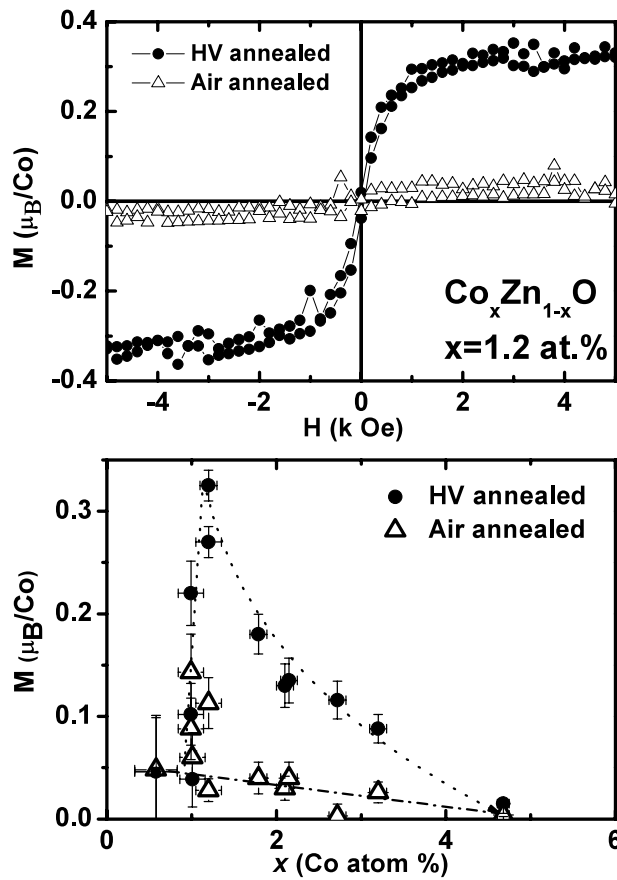


**Figure 3.** Upper panel:  $M$  versus  $H$  at 300 K for  $\text{Co}_{0.012}\text{Zn}_{0.988}\text{O}$  after high-vacuum annealing (solid symbol) and air annealing (open symbols). Lower panel: magnetic moment per  $\text{Co}^{2+}$  in  $\text{Zn}_{1-x}\text{Co}_x\text{O}$  thin films annealed in air and high vacuum as a function of  $x$ . The dashed and dash-dot lines are a guide to the eye.

in saturation magnetization with Co concentration. This behaviour is qualitatively similar to what has been observed previously in  $\text{Co}:\text{SnO}_2$  [9].

The air annealed  $\text{Co}:\text{ZnO}$  films show a small magnetic moment of  $\sim 0.04 \mu_B/\text{Co}$  for the smallest value of  $x$  measured ( $x = 0.5\%$ ). This moment tends to decrease with increasing  $x$ , as illustrated by the dot-dashed line in the lower panel of figure 3, with the exception of large fluctuations close to  $x = 1.2\%$ . This particular Co concentration corresponds to the sharp increase in the magnetic moment of the HV annealed films. We attribute the enhanced air-annealed moment at  $x = 1.2\%$  to fluctuations associated with the incomplete percolation of bound magnetic polarons. The decrease in magnetic moment with increasing  $x$  may arise from the formation of an antiferromagnetic spinel  $\text{Zn}_y\text{Co}_{3-y}\text{O}_4$  secondary phase [18].

When annealed in high vacuum, the samples show a large increase in magnetic moment. The highest magnetic moment of  $\sim 0.3 \mu_B/\text{Co}$  is observed for  $\text{Zn}_{0.988}\text{Co}_{0.012}\text{O}$  film, which is small in comparison to the full  $\text{Co}^{2+}$  moment ( $3 \mu_B$ ), and also smaller than some previously reported values [8]. This dramatic increase in the magnetization of the films occurs simultaneously with the elimination of the  $690 \text{ cm}^{-1}$  Raman peak, which allows the

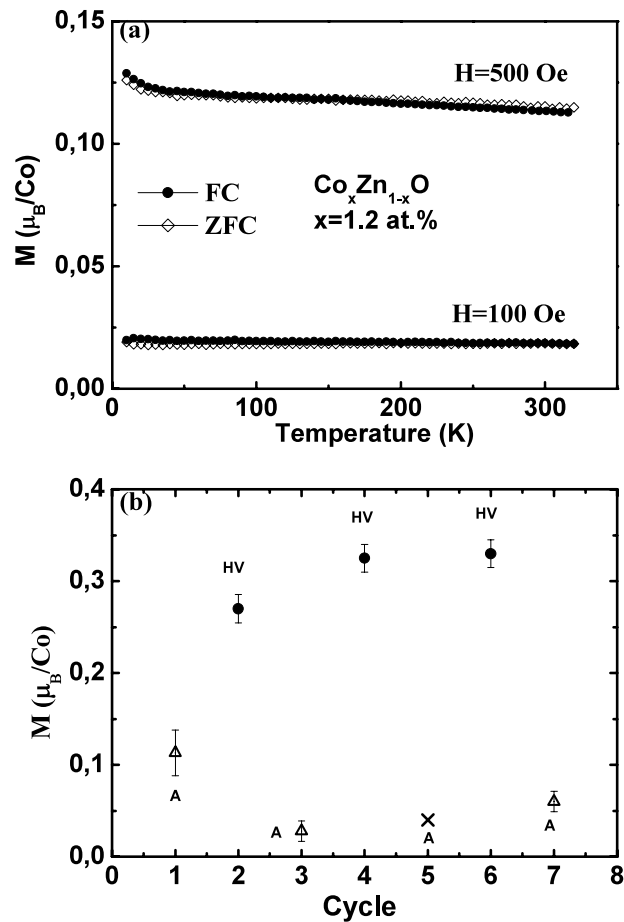


**Figure 4.** (a) Temperature versus magnetization curves in zero-field cooled (ZFC) and field cooled (FC) conditions of vacuum-annealed sample. (b) Magnetic moment per  $\text{Co}^{2+}$  in  $\text{Co}_{0.012}\text{Zn}_{0.988}\text{O}$  on repeated annealing in air and high vacuum. ( $\bullet$ —HV annealed;  $\Delta$ —air annealed;  $\times$ —after air annealing cycle, the magnetic moment was not measured.)

possibility of a relationship between the magnetic properties and lattice structural properties of the samples. The possibility of an enhanced magnetic moment arising from the reduction of  $\text{Co}^{2+}$  to metal clusters has been excluded for the following reasons: if the metal clusters were to form in ZnO, the characteristic optical absorption peaks of  $\text{Co}^{2+}$  in the optical spectra would have reduced intensities. Furthermore, with the formation of metal clusters one would expect an increase in the magnitude of the magnetic moment with increasing Co concentration, contrary to the observations (figure 3). Finally, we found no difference between the zero-field cooled and the field cooled magnetization curves, which further suggests that the magnetism in Co-doped ZnO films does not result from the superparamagnetic behaviour associated with magnetic nanoparticles (figure 4(a)). The origin of the decrease in magnetization for the HV-annealed samples at larger values of  $x$  is unclear. Raman spectroscopy shows no evidence for  $\text{Zn}_x\text{Co}_{3-x}\text{O}_4$  clusters in these samples. At a higher concentration of Co, it is possible that the decrease in magnetic moment arises from increasing antiferromagnetic interactions between Co ions in close proximity in the lattice.



The magnetization of the  $\text{Zn}_{1-x}\text{Co}_x\text{O}$  samples is very sensitive to the HV annealing treatment. Figure 4(b) shows the saturation magnetization on repeated air and vacuum annealing cycles. With the first vacuum annealing, the magnetic moment increased from 0.1 to  $0.27 \mu_{\text{B}}/\text{Co}$ . Subsequently, annealing the sample in air is found to lower the magnetization ( $\sim 0.02 \mu_{\text{B}}/\text{Co}$ ), while again reannealing the sample in vacuum increases the magnetization. This is qualitatively what one would expect for bound magnetic polaron induced ferromagnetism, where the presence of oxygen vacancies is crucial for developing ferromagnetic order in semiconducting oxides. The present results are distinct from the previous report of Kittilsved *et al* [22, 23], where they demonstrated a reversible 300 K ferromagnetic ordering in Co:ZnO by lattice incorporation and removal of the native n-type Zn interstitial defect. Our previous measurements on Co:TiO<sub>2</sub> and Fe:TiO<sub>2</sub> also showed a substantial enhancement of FM on HV annealing [24, 25]. A similar observation in Co:TiO<sub>2</sub> has been reported by Griffin *et al* [20], however no reversible switching behaviour has been demonstrated. Further investigation on the possible role played by the secondary impurity phase in contributing to the measured moment is required before the observed ferromagnetic order can be attributed unambiguously to  $\text{Co}^{2+}$ /oxygen vacancy effects. In fact, preliminary results on  $\text{Co}_{3-y}\text{Zn}_y\text{O}_4$  thin films indicate a similar enhancement in the magnetization under high-vacuum annealing [26].

The sudden onset of a large ferromagnetic moment with increasing Co concentration, as shown in the lower panel of figure 3, is consistent with the percolative transition proposed in the bound magnetic polaron model. In this picture, an electron associated with a particular defect is confined in a hydrogenic orbital of radius  $r_{\text{H}} = \epsilon(m/m^*)a_0$ , where  $\epsilon$  is the dielectric constant,  $m$  is the electron mass,  $m^*$  is the effective mass of the donor electrons, and  $a_0$  is the Bohr radius (0.53 Å) [9]. Motivated by figure 4, we argue that vacuum annealing the Co:ZnO films always introduces a sufficient concentration of oxygen vacancy defects to form a percolative polaron chain, so that the development of ferromagnetic order is limited by the concentration of magnetic ions rather than the defect concentration. At low values of  $x$  we suppose that the moment is small because there is an insufficient Co concentration to produce a net magnetization in each polaron in the chain. Once  $x$  increases past 1.2% ( $5 \times 10^{26} \text{ Co m}^{-3}$ ), there is a dramatic increase in the saturation magnetization, which we attribute to the development of a net moment on each percolative polaron. Using the simplistic assumption that this occurs when there is precisely one Co ion in each percolative polaron, and that the Co ions are distributed uniformly, we estimate the effective size of the magnetic polarons to be 7.8 Å. This value is close to the predicted polaron size of 7.6 Å in ZnO [9], although we emphasize that our estimate is based on the inferred magnetization of the polarons rather than on a direct measure of defect concentration.

In summary, we have demonstrated the existence of a disordered  $-\text{Zn}-\text{O}-\text{Co}-$  local vibrational Raman active mode  $\sim 690 \text{ cm}^{-1}$  in  $\text{Co}_x\text{Zn}_{1-x}\text{O}$  films. This mode disappears upon vacuum annealing and reappears upon air annealing. The reproducible behaviour of this local vibrational mode strongly suggests the formation of oxygen vacancies ( $-\text{Zn}-\square-\text{Co}-$ ) upon vacuum annealing. While air-annealed  $\text{Co}_x\text{Zn}_{1-x}\text{O}$  films show weak ferromagnetism at room temperature, upon vacuum annealing the magnetic moment is greatly enhanced, reaching a maximum value at  $x \sim 0.012$ . The dependence of the magnetic moment on oxygen vacancies, deduced from Raman measurements, is consistent with the bound magnetic polaron model of ferromagnetism in diluted magnetic semiconducting oxides (DMSO). Making assumptions consistent with the bound magnetic polaron model for FM in DMSO systems, we find an effective polaron radius of 7.8 Å in Co:ZnO. However, the presence of a secondary  $\text{Zn}_y\text{Co}_{3-y}\text{O}_4$  impurity phase at larger values of Co concentration precludes us from definitively attributing the observed ferromagnetic order to intrinsic effects.

## References

- [1] Özgür Ü, Alivov Ya I, Liu C, Teke A, Reshchikov M A, Doğan S, Avrutin V, Cho S-J and Morkoç H 2005 *J. Appl. Phys.* **98** 041301
- [2] Chambers S A and Yoo Y K (ed) 2003 Reviews compiled in *MRS Bull.* **23** 706
- [3] Dietl T, Ohno H, Matsukura F, Cibert J and Ferrand D 2000 *Science* **287** 1019
- [4] Ueda K, Tabata H and Kawai T 2001 *Appl. Phys. Lett.* **79** 988
- [5] Lee H J, Jeong S Y, Cho C R and Park C H 2002 *Appl. Phys. Lett.* **81** 4020
- [6] Prellier W, Fouchet A, Mercey B, Simon Ch and Raveau B 2003 *Appl. Phys. Lett.* **82** 3490
- [7] Norton D P, Overberg M E, Pearton S J, Prussner K, Budai J D, Boatner L A, Chisholm M F, Lee J S, Khim Z G, Park Y D and Wilson R G 2003 *Appl. Phys. Lett.* **83** 5488
- [8] Venkatesan M, Fitzgerald C B, Lunney J G and Coey J M D 2004 *Phys. Rev. Lett.* **93** 177206
- [9] Coey J M D, Venkatesan M and Fitzgerald C B 2005 *Nat. Mater.* **4** 173
- [10] Dietl T 2003 *Nat. Mater.* **2** 646
- [11] Bundesmann C, Ashkenov N, Schuber M, Spemann D, Butz T, Kaidashev E M, Lorents M and Grundmann M 2003 *Appl. Phys. Lett.* **83** 1974
- [12] Nickel N H, Friedrich F, Rommeluère J F and Faltier P 2005 *Appl. Phys. Lett.* **87** 211905
- [13] Manjón F J, Mari B, Serrano J and Romero A H 2005 *J. Appl. Phys.* **97** 053516
- [14] Koidl P 1977 *Phys. Rev. B* **15** 2493
- [15] Srikant V and Clarke D R 1997 *J. Appl. Phys.* **81** 6357
- [16] Serrano J, Romero A H, Manjón F J, Lauck R, Cardona M and Rubio A 2004 *Phys. Rev. B* **69** 094306
- [17] Ohtsuka H, Tabata T, Okada O, Sabatino L M F and Bellussi G 1997 *Catal. Lett.* **44** 265
- [18] Samanta K, Bhattacharya P, Katiyar R S, Iwamoto W, Pagliuso P G and Rettori And C 2006 *Phys. Rev. B* **73** 245213
- [19] Merlin R, Pinczuk A and Weber W H 2000 *Raman Scattering in Materials Science* vol 1, ed W H Weber and R Merlin (Berlin: Springer) p 19
- [20] Griffin K A, Pakhomov A B, Wang C M, Heald S M and Krishnan K M 2005 *J. Appl. Phys.* **97** 10D320
- [21] Weng H, Yang X, Dong J, Mizuseki H, Kawasaki M and Kawazoe Y 2004 *Phys. Rev. B* **69** 125219
- [22] Kittilstved K R, Schwartz D A, Tuan A C, Heald S M, Chambers S A and Gamelin D R 2006 *Phys. Rev. Lett.* **97** 037203
- [23] Schwartz D A and Gamelin D R 2004 *Adv. Mater.* **16** 2115
- [24] Suryanarayanan R, Naik V M, Kharel P, Talagala P and Naik R 2005 *J. Phys.: Condens. Matter* **17** 755
- [25] Suryanarayanan R, Naik V M, Kharel P, Talagala P and Naik R 2005 *Solid State Commun.* **133** 439
- [26] Sudakar C *et al* 2007 *J. Appl. Phys.* submitted